INVESTIGACIÓN
E INNOVACIÓN
EN INGENIERÍAS

Comparative assessment of machine learning techniques for fault-induced voltage sag classification

Evaluación comparativa de técnicas de aprendizaje automático para la clasificación de huecos de tensión inducidos por fallas

Joaquín Caicedo Navarro
Edwin Rivas Trujillo
Universidad Distrital Francisco José de Caldas, Colombia

OPEN ACCESS

Received:
16/12/2024
Accepted:
24/03/2025
Published:
21/05/2025

Correspondence:
aalvarez@unicauca.edu.co

DOI:
https://doi.org/10.17081/invinno.13.1.7565

Abstract
Objective: To compare various artificial intelligence techniques for classifying fault-induced voltage sags using quantitative and qualitative criteria, alongside the analytic hierarchy process. **Methodology:** Extensive synthetic signals of fault-induced voltage sags were generated using MATLAB/Simulink simulations. Feature engineering included the application of transformations such as the space phasor model, discrete Fourier transform, and short-time Fourier transform. These transformations enabled the extraction of time-series, spectral, and statistical features from the signals, generating ten different feature sets. The most relevant features were then selected using several algorithms to optimize classification performance. Decision trees, support vector machines, and artificial neural networks were employed for classification, with performance evaluated based on computation time, storage requirements, accuracy, and interpretability. The analytic hierarchy process was applied to assess the overall suitability of each approach. **Results:** Decision trees demonstrated speed, accuracy, and high interpretability, making them ideal for real-time applications. Support vector machines also achieved good accuracy but required more resources and had moderate interpretability. Artificial neural networks offered balanced performance with limited interpretability. **Conclusions:** Among the evaluated algorithms, decision trees are the most suitable for real-time classification of fault-induced voltage sags. However, the choice of technique should align with specific application needs. Future research should consider additional criteria and focus on improving interpretability through explainable artificial intelligence techniques.

Keywords: Machine learning, decision tree, feature engineering, electrical system failure, voltage sag, support vector machine, Artificial Neural Network (ANN).

Resumen
Objetivo: Comparar diversas técnicas de inteligencia artificial para clasificar huecos de tensión inducidos por fallas utilizando criterios cuantitativos y cualitativos, junto con el proceso analítico jerárquico. **Metodología:** Se generaron señales sintéticas de huecos de tensión mediante simulaciones en MATLAB/Simulink. La ingeniería de características incluyó transformaciones como el modelo de fasor espacial, la transformada de Fourier discreta y la de tiempo corto. Estas transformaciones permitieron extraer características temporales, espectrales y estadísticas, generando diez conjuntos diferentes. Las características principales fueron seleccionadas mediante algoritmos para optimizar la clasificación. Se utilizaron árboles de decisión, máquinas de vectores de soporte y redes neuronales artificiales, evaluando su rendimiento en función del tiempo de cálculo, requisitos de almacenamiento, precisión e interpretabilidad. El proceso analítico jerárquico se aplicó para evaluar la idoneidad general de cada enfoque. **Resultados:** Los árboles de decisión demostraron ser rápidos, precisos y altamente interpretables, lo que los hace ideales para aplicaciones en tiempo real. Las máquinas de vectores de soporte también lograron buena precisión, pero requirieron más recursos y presentaron una interpretabilidad moderada. Las redes neuronales artificiales ofrecieron un rendimiento equilibrado con una interpretabilidad limitada. **Conclusiones:** Entre los algoritmos evaluados, los árboles de decisión son los más adecuados para la clasificación en tiempo real de huecos de tensión. Sin embargo, la elección de la técnica debe alinearse con las necesidades específicas de la aplicación. Investigaciones futuras deberían considerar criterios adicionales y centrarse en mejorar la interpretabilidad mediante técnicas de inteligencia artificial explicable.

Palabras claves: Aprendizaje automático, árbol de decisión, ingeniería de características, falla en el sistema eléctrico, hueco de tensión, máquina de v

ectores soporte, Red Neuronal Artificial (RNA).

How To Cite (IEEE): J. Caicedo Navarro and E. Rivas Trujillo “Comparative assessment of machine learning techniques for fault-induced voltage sag classification.”, Investigación e Innovación en Ingenierías, vol. 13, no. 1, pp. 60–81, 2025. DOI: https://doi.org/10.17081/invinno.13.1.7565

Introduction

Power Quality (PQ) refers to the characteristics of electricity at specific points in an electrical system, evaluated against set reference parameters [1, 2]. Deviations from these parameters, known as PQ Disturbances (PQDs), can impact system users and are typically categorized as voltage or current quality issues [3]. The severity of PQDs can lead to energy inefficiency, equipment malfunction, and disruptions in industrial processes [4, 5], and subsequent financial losses incurred by utilities and end users [6].

Voltage sags, or dips, are significant due to their potential to cause equipment failures. These sags involve a reduction in root mean square (rms) voltage from 0.1 to 0.9 per unit (pu) and can last from half a cycle to one minute. They are typically caused by faults but can also result from events like transformer energizing, motor starting, and heavy load switching [7]. Proper classification of fault-induced voltage sags is essential for the effective operation of protection systems, as different fault types (e.g., three-phase, two-phase to ground) produce distinct disturbance patterns [8, 9].

Detection and classification of PQDs, particularly voltage sags, are essential in modern power systems, especially with the rise of smart grids and the proliferation of power electronic devices, which are highly sensitive to PQDs [10, 11]. Detection aids in identifying the timing and location of voltage and current deviations, while classification assists in pinpointing the type and source of disturbances and in selecting suitable mitigation strategies. In addition, real-time monitoring systems offer synchronized, continuous, and single- or multipoint measurements that enable the analysis of PQD propagation and the accurate and prompt decision-making to address PQ issues [1, 12].

The detection and classification of voltage sags, both offline and in real-time, have been extensively explored through various approaches. Transformation such as Discrete Fourier Transform (DFT) [10], Short-Time Fourier Transform (STFT) [5], Wavelet Transform (WT) [13], Stockwell Transform (ST) [14], Space Phasor Model (SPM) [15, 16], Phase Space Reconstruction (PSR) [17] have been employed in the feature engineering stage prior to classification. Various features have been extracted from these transformations for voltage sag classification, including statistical [18, 19], time series [20], [21], image-based [9, 15, 22], and spectral features [23], each offering specific advantages depending on the application and classification tools.

The most widely used Artificial Intelligence (AI) methods for voltage sag classification in the literature include Artificial Neural Networks (ANN) [24], Decision Trees (DT) [25], and Support Vector Machines (SVM) [26]. Other relevant AI techniques, such as fuzzy logic [27], k-Nearest Neighbors (kNN) [28], and deep learning algorithms [11, 29], have also been applied. Despite the development of numerous structured methodologies for voltage sag detection and classification, research gaps remain, particularly in the reliability of indices for classifying real-world (field) voltage sags in real-time and the physical interpretation of AI-based classification results [1, 30].

Given the extensive availability of AI-based tools for automatic classification, selecting the most suitable one, as well as fine-tuning and training these models for specific applications, presents a complex challenge [31–34]. The study in [8] introduces a set of metrics to compare various transformations and feature extraction techniques. Building on this work, our research extends the analysis to evaluate and compare the performance of several AI-based classifiers using these features as inputs, following a feature selection process. Moreover, a systematic approach to this process is proposed based on the Analytic Hierarchy Process (AHP).

In this context, this study implements different AI-based tools for classifying fault-induced voltage sags, including variants of DT, SVM, ANN. The goal is to demonstrate the strengths and limitations of the most used approaches, offering the following contributions:

- Formulation of quantitative and qualitative metrics, such as computation time, storage requirements, accuracy, and interpretability, for systematic assessment.

- A comprehensive methodology for evaluating the suitability of different approaches using the AHP.

The proposed methodology is applied to a case study for real-time applications, but it is flexible enough to accommodate various needs by adjusting metric weights. The paper is structured as follows: Section 2 reviews comparison approaches and AI-based voltage sag classifiers; Section 3 outlines the comparison methodology; Section 4 presents application results; and Section 5 concludes the study.

Related works

Comparison approaches of PQD classification

Several studies have investigated various methods to compare and assess classification techniques for voltage sag detection and classification, particularly focusing on AI-based approaches. For example, the study in [31] introduces a method using subcomponent features with machine learning algorithms such as random forest, LightGBM, kNN, and XGBoost. This approach demonstrates high accuracy and efficiency, even under noisy conditions, highlighting the importance of feature selection and optimization for reliable results. Similarly, [32] compares wavelet transforms for feature extraction, evaluating classifiers including DT, SVM, and kNN. SVM is identified as the most accurate, though further optimization is needed for better PQD classification.

In addition, [33] examines deep learning models, including Convolutional Neural Networks (CNN), Long Short-Term Memory (LSTM) networks, and hybrid CNN-LSTM models, finding that hybrid CNN-LSTM models offer superior classification accuracy compared to standalone CNN or LSTM models, especially with real-world measurements. Furthermore, [34] proposes a hybrid approach combining the ST with kNN, DT, and SVM, and employs optimization techniques like genetic algorithms and Competitive Swarm Optimization (CSO). This ST-based CSO-SVM model is noted for its robustness against noise, making it highly effective for real-world PQD classification.

From the literature reviewed, it is evident that most comparison approaches focus primarily on accuracy as a single metric, with some consideration of reliability in noisy environments. However, given the diverse applications of these tools, such as real-time PQD mitigation, off-line data categorization, and trend analysis, a more comprehensive and multidimensional assessment of classification tools is essential.

AI methods for voltage sag classification

Given that the most widely used AI methods for voltage sag classification include ANN, DT, and SVM [1], this article focuses on these tools. Each method offers unique advantages and challenges, making their comparative analysis crucial for understanding their suitability in different scenarios.

DT are knowledge-based systems developed through inductive inference, providing simplicity, efficiency, and clear physical interpretation, which are beneficial for real-time applications. Despite their widespread use for classifying various PQDs, DT are less commonly applied to voltage sag classification. Some variants such as random forest have been used and they are often employed in ensemble models, serving as weak classifiers combined with other methods [28, 35, 36].

SVM are robust supervised learning models used for classification and regression. They function by maximizing the margin between classes, which makes them effective even with limited training data, an advantage in PQD detection and classification. SVM have been extensively applied to PQD and voltage sag classification [36–38]. Variants of SVM, such as multiclass SVM [39], least square SVM [40], rank SVM [41], and directed acyclic graph SVM [42], further expand their application.

ANN are computational models inspired by the human brain, consisting of interconnected neurons that process signals through weights. They are capable of modeling complex nonlinear functions with extensive operations. Shallow ANN, including input, hidden, and output layers, are used for classification tasks. Various shallow ANN, such as learning vector quantization [43], probabilistic neural networks [44], radial basis functions [45], multilayer perceptron [46], feedforward networks [47], backpropagation networks [48], and extreme learning machines [49], are used for voltage sag and multiple PQD classification.

Methodology

As outlined in [1], the comprehensive approach to monitoring and analyzing PQDs involves four primary stages: (i) input space, (ii) preprocessing, (iii) feature engineering, and (iv) decision space. Each stage encompasses specific steps: 1. input data preparation (i), 2. data preprocessing (ii), 3. transformation (iii), 4. feature extraction (iii), 5. feature selection (iii), 6. detection (iv), 7. classification (iv), and 8. characterization (iv). It is worth noting that not all steps are mandatory in every scenario, allowing the framework to be flexible and adaptable to a variety of applications.

In [8], steps 1 through 4 are addressed for the characterization of fault-induced voltage sags, including a comparative analysis of various transformations and feature extraction methods. Building on those preliminary results, and with some adaptations as described later, this study focuses on implementing feature selection techniques and AI-based classifiers, specifically steps 5 and 7, to perform the classification. A comparative analysis of these classifiers is then conducted using a proposed AHP-based approach.

The complete methodology for executing these stages and comparing different classifiers is illustrated in Figure 1.

Figure 1. Combinations of applied approaches for voltage sag classification

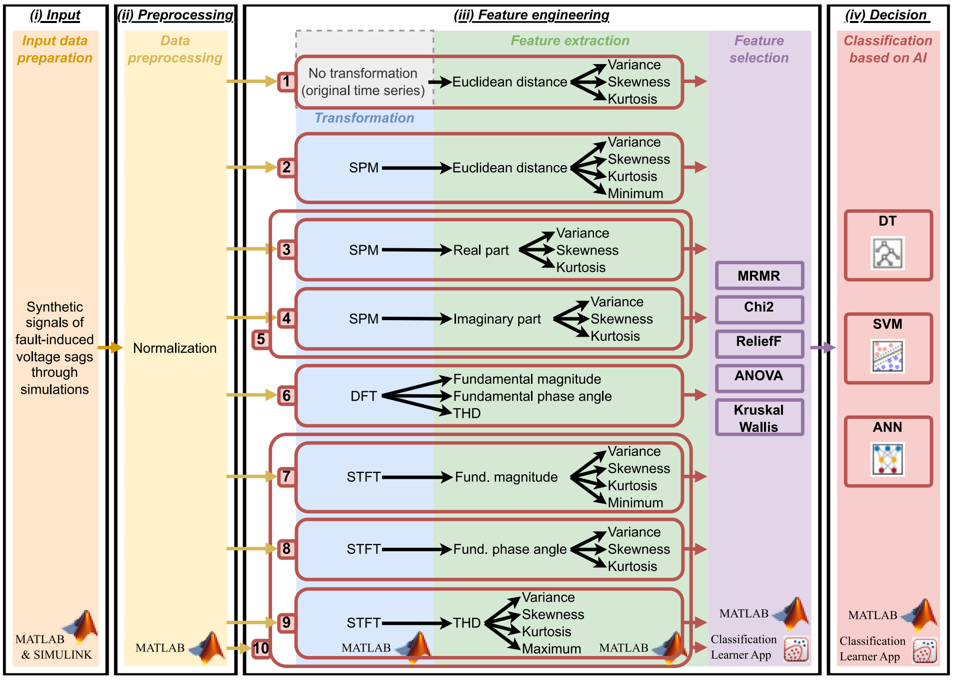

Source: own elaboration

Input data preparation and preprocessing

In the initial step, synthetic time-domain discrete signals are generated by simulating fault-induced voltage sags using the Simulink model shown in Figure 2, and a MATLAB script is used to systematically conduct the simulations, as outlined in [8]. Ten types of voltage sags are simulated, corresponding to the fault types listed in Table 1. For each fault type, 100 simulations are performed, varying the fault location and duration randomly along Line 1, resulting in a total of 1,000 simulations. Consequently, a dataset comprising 3,000 voltage signals (1,000 per phase) is produced. Each voltage signal covers 10 cycles at 60 Hz, sampled at a frequency of 60 kHz (with a 10-μs time step), resulting in 10,000 discrete values per signal. The voltage signals are then normalized and expressed in per unit (pu) for consistency.

To further assess the classifiers' performance, random white Gaussian noise is introduced to the signals, simulating a noisy environment. The Signal-to-Noise Ratio (SNR) is set at 50 dB, a value commonly used in literature [10, 14] to evaluate the reliability of PQD classifiers under simulated conditions.

Figure 2. Scheme implemented in Simulink for voltage sag simulation

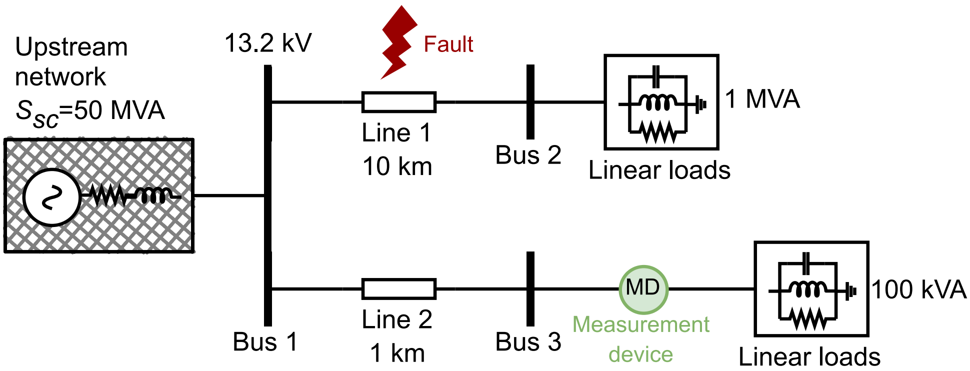

Source: adapted from [8].

Table 1. Classification of voltage sags according to the fault type

Fault type	Voltage sag type
Three-phase	abcG
Two-phase to ground (phases a, b)	abG
Two-phase to ground (phases a, c)	acG
Two-phase to ground (phases b, c)	bcG
Two-phase (phases a, b)	ab
Two-phase (phases a, c)	ac
Two-phase (phases b, c)	bc
Single-phase to ground (phase a)	aG
Single-phase to ground (phase b)	bG
Single-phase to ground (phase c)	cG

Source: adapted from [8]

Transformation and feature extraction

Transformations, including SPM, DFT, and STFT, are implemented in MATLAB and applied to the signals as outlined in [8]. Subsequently, a variety of statistical, time-series, and spectral features are computed from the transformation coefficients. Additionally, features are extracted directly from the original time-series signals to evaluate the outcomes without any transformation. The combinations of applied transformations and extracted features, along with their graphical representation for clarity, are summarized in the feature engineering process depicted in Figure 2. This figure outlines the foundational work detailed in [8], where more comprehensive information can be found.

Beyond the feature sets developed in [8], new sets (3, 4, and 5) are proposed in this study to enhance the classification performance of the SPM. These sets are designed by extracting statistical indices from both the real and imaginary parts of the transformation.

Figure 3. Applied transformations and feature extraction techniques

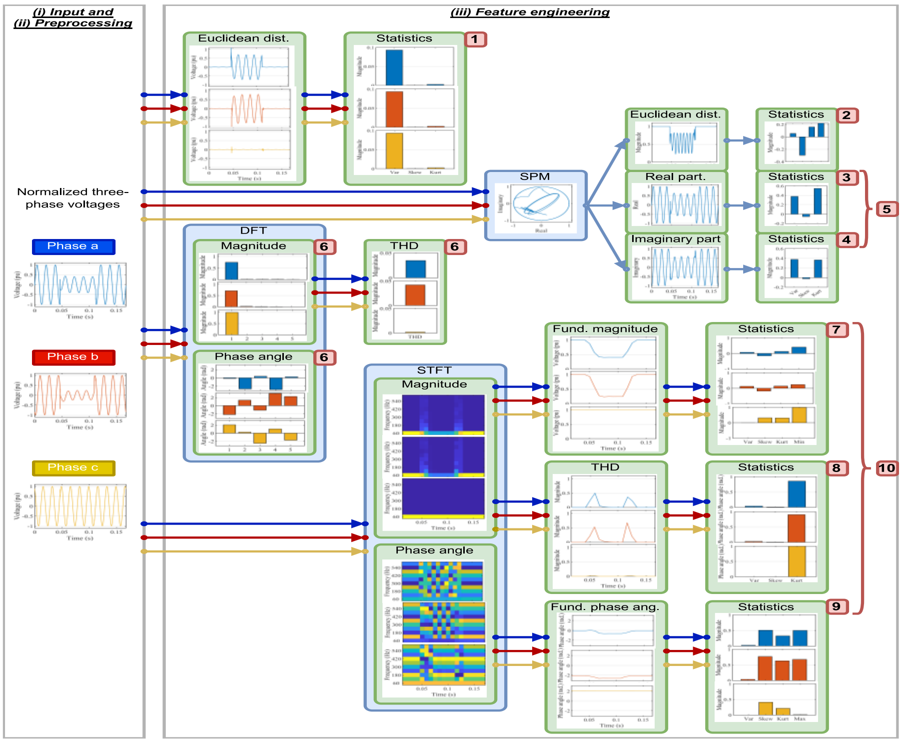

Source: own elaboration

Feature selection

After generating the feature sets, a feature selection process is implemented to optimize the trade-off between the number of features and classification accuracy. This process is carried out using MATLAB's Classification Learner App, which applies several algorithms:

- Minimum Redundancy Maximum Relevance (MRMR): This algorithm sequentially selects features that minimize redundancy and maximize relevance, enhancing the efficiency of the model.

- Chi-square: This approach tests each predictor's independence from the response variable through individual chi-square tests, ranking features based on their p-values, with lower p-values indicating greater significance.

- ReliefF: The ReliefF algorithm ranks features by evaluating their importance in supervised models that utilize distance metrics, focusing on the proximity between pairs of observations to estimate feature relevance.

- Analysis of Variance (ANOVA): ANOVA performs a one-way analysis of variance for each predictor variable, grouping them by class and ranking features according to the p-values derived from the test statistics.

- Kruskal Wallis: This method ranks features using p-values from the Kruskal-Wallis test, assessing whether the medians of the populations from which grouped predictor values are drawn are statistically equivalent.

The feature selection process is systematically applied to each of the ten feature sets (see Figure 2) using these algorithms. Features consistently receiving the lowest rankings across the six selection methods are candidates for elimination. However, this elimination is critically evaluated on a case-by-case basis, ensuring that essential features are not discarded. These methods provide a comprehensive toolkit for refining the feature set, ultimately improving the classification model's performance.

Classification

Subsequently, fault-induced voltage sags are classified in the decision space using AI-based tools such as DT, SVM, and ANN. These classifiers are implemented within MATLAB's Classification Learner App, utilizing the coefficients derived from each of the ten feature engineering approaches. During the training phase, each feature engineering approach is paired with a set of selected features obtained through various feature selection algorithms as described above. This process results in the development of three classifiers, DT, SVM, and ANN, for each feature engineering approach.

Framework for comparison

The classification methods for voltage sags result in a total of 30 different approaches, encompassing three types of classifiers (DT, SVM, and ANN), each trained with 10 distinct feature sets. The effectiveness of these classifiers is assessed through both quantitative and qualitative metrics, as shown in Figure 4. These metrics are further elaborated below:

- **Computation time:** This metric includes both the training and prediction phases. Additionally, prediction time can be further divided into the time required for feature engineering and the time for classification.
- **Storage requirements:** This parameter refers to the amount of memory needed to store the models and their respective parameters, particularly important for real-time or embedded applications where resources may be limited. Moreover, the number of required input features is also directly related to storage needs.
- **Accuracy:** This aspect evaluates the precision of the classifiers in correctly identifying the type of fault-induced voltage sag. It is one of the most critical performance metrics, as higher accuracy leads to more reliable fault detection and classification.
- **Interpretability:** This criterion assesses how easily the results can be interpreted and whether they provide a clear, physical explanation of the phenomena. Key aspects of interpretability include simplicity, transparency, and consistency of the results.

Figure 4. Performance metrics for comparing AI-based classifiers.

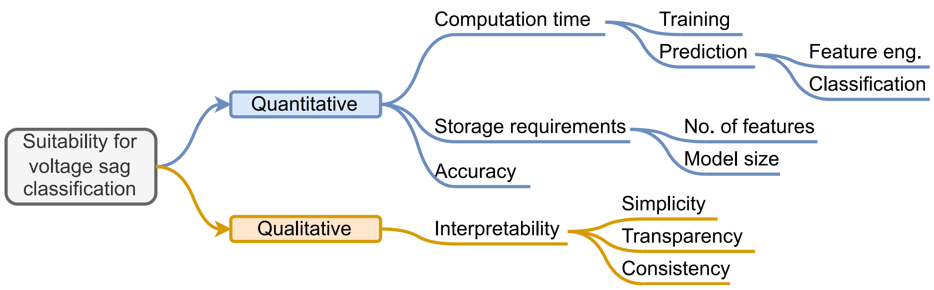

Source: own elaboration

To quantify the overall suitability of the classifiers for voltage sag classification, the AHP is employed. The AHP assigns weights to each of the quantitative and qualitative aspects, resulting in a final score for each method. These weights can be adjusted based on the specific requirements of the application under consideration. For instance, in real-time applications, computation time and storage requirements might be given greater emphasis. In such cases, computation time is critical for achieving real-time performance, while storage requirements are essential for potential implementation in dedicated hardware.

Results

This section presents and discusses the outcomes of the feature selection (step 5) and classification (step 7) processes, along with an AHP-based comparison of the methods. The selected features, as determined by the feature selection process, are summarized in Table 2.

Table 2. Set of selected features

Original feature engineering approach	Transf.	Selected features 1 (Time-domain and spectral)	Selected features 2 (Statistical)	Total of selected features*
1: No transf. + Euclidean distance + (variance, skewness, kurtosis)	--	Euclidean distance	Variance	6/9
			Kurtosis	
2: SPM + Euclidean distance + (variance, skewness, kurtosis, min)	SPM	Euclidean distance	Variance	4/4
			Skewness	
			Kurtosis	
			Minimum	
3: SPM + real part + (variance, skewness, kurtosis)	SPM	Real part	Variance	3/3
			Skewness	
			Kurtosis	
4: SPM + imaginary part + (variance, skewness, kurtosis)	SPM	Imaginary part	Variance	3/3
			Skewness	
			Kurtosis	
5: 3 and 4	SPM	Real part	Variance	4/6
			Kurtosis	
		Imaginary part	Variance	
			Kurtosis	
6: DFT + (fund. magnitude, fund. phase angle, THD)	DFT	Fund. mag.	--	6/9
		Fund. phase	--	
7: STFT + fund. magnitude + (variance, skewness, kurtosis, min)	STFT	Fund. mag.	Minimum	3/12
8: STFT + fund. phase + (variance, skewness, kurtosis)	STFT	Fund. phase	Variance	6/9
			Kurtosis	
9: STFT + THD + (variance, skewness, kurtosis, max)	STFT	THD	Skewness	6/12
			Maximum	
10: 7, 8, and 9	STFT	Fund. mag.	Minimum	6/33
		THD	Maximum	

* Number of selected features over the total number of features of the original approach.

Source: own elaboration

Results in Table 2 show that, in most approaches, statistical features are calculated for each phase of the voltage signal. For example, in the first feature engineering approach, variance and kurtosis of the Euclidean distance for each phase are identified as relevant features, resulting in a total of six selected features (variance and kurtosis for each of the three phases).

In contrast, when the SPM is employed as the transformation, the three-phase signals are consolidated into a single signal. Consequently, statistical metrics are computed only for this unified signal. As an illustration, in feature engineering approach 2, four features are selected: variance, skewness, kurtosis, and the minimum value of the Euclidean distance of the SPM.

It is also noteworthy that feature engineering approaches incorporating SPM (approaches 2 through 4) retain all original features to maximize accuracy. Conversely, some approaches lead to significant dimensionality reduction. For instance, in approach 7, only three features are selected out of 12, and in approach 10, only six out of 33 are chosen, highlighting the substantial reduction in feature space.

Furthermore, Table 3 summarizes the classification results, highlighting the quantitative performance metrics introduced in the previous section: computation time, storage requirements, and accuracy.

Table 3. Summary of quantitative metrics of the classifiers

Feature set (with selected features)	Classifier	Computation time				Storage		Accuracy (%)
		Training (s)	Prediction (ms)			No. features	Size (KB)	
			Feat. eng.	Clas.	Total			
1	DT	2.42	1.48	0.01	1.49	6	11	100
	SVM	4.99		0.11	1.59		261	99.3
	ANN	1.76		0.01	1.49		13	100
2	DT	1.87	1.00	0.01	1.01	4	54	27.3
	SVM	2.81		0.12	1.12		208	28.7
	ANN	9.86		0.04	1.04		10	33.0
3	DT	1.22	0.95	0.01	0.96	3	16	44.3
	SVM	54.31		0.13	1.08		301	47.3
	ANN	9.77		0.01	0.96		12	49.7
4	DT	2.58	0.94	0.01	0.95	3	53	48.0
	SVM	1.90		0.19	1.13		359	50.7
	ANN	6.34		0.01	0.95		12	54.7
5	DT	2.08	1.05	0.01	1.06	4	47	86.0
	SVM	5.22		0.11	1.16		241	90.3
	ANN	10.86		0.02	1.07		19	91.7
6	DT	2.32	0.80	0.01	0.81	6	11	99.3
	SVM	3.65		0.05	0.85		223	100
	ANN	1.33		0.02	0.82		9	100
7	DT	2.13	2.89	0.01	2.90	3	20	97.3
	SVM	4.98		0.08	2.97		213	100
	ANN	1.49		0.01	2.90		9	100
8	DT	2.26	2.97	0.01	2.98	6	11	99.7
	SVM	5.40		0.07	3.04		247	99.0

	ANN	3.01		0.01	2.98		9	99.3
9	DT	2.36	3.16	0.01	3.17	6	11	99.3
	SVM	1.73		0.08	3.24		300	100
	ANN	3.10		0.01	3.17		11	98.0
10	DT	2.36	3.15	0.01	3.16	6	11	100
	SVM	2.07		0.10	3.25		224	100
	ANN	1.03		0.01	3.16		11	100

Source: own elaboration

Computation time

Table 3 outlines the median computation times from 100 training iterations per classifier, executed on a CPU with a six-core processor (2.20 GHz, 12 GB RAM). The data reveals significant differences in training and prediction times across various approaches. DT and ANN classifiers consistently exhibit low prediction times, making them highly advantageous for real-time applications. A key observation is that the prediction time is largely dictated by the duration of the feature engineering process. Approach 6 excels with the shortest feature engineering time of just 0.8 ms, positioning it as the most efficient option for time-sensitive tasks.

Storage requirements

The storage demands for each classifier, as detailed in Table 3, highlight the memory footprint associated with different approaches. For example, the DT and ANN models from approach 1 require just 11 KB, and 13 KB, respectively, while the SVM model for the same feature set demand 261 KB. This comparison underscores the storage efficiency of DT and ANN, which is especially important when deploying models on resource-constrained devices. In contrast, SVM models generally require more storage due to their higher complexity and parameter count.

Accuracy

Classifier accuracy was assessed using holdout validation, with 70% of the data allocated for training and 30% for testing. The accuracy metrics in Table 3 reveal that, except for SPM-based approaches (2-4), all classifiers achieve high accuracy rates. This evaluation is crucial for understanding the generalization capabilities of each model. Although SPM-based methods initially show reduced accuracy, the integration of statistical metrics for both real and imaginary components in approach 5 yields improved results, though it still falls short compared to other methods. Overall, DT, SVM, and ANN classifiers perform well in terms of accuracy, making them robust choices for this application.

Interpretability

Feature interpretability is crucial for gaining a better understanding of the voltage sag phenomenon, facilitating more effective applications of the analysis. Clear thresholds for features allow for a better understanding of the range of each sag category. In this regard, DT and SVM provide more defined thresholds, with DT being simpler to apply. Conversely, ANN models are more complex, and no easy interpretation is given to the internal process and decision boundaries.

To illustrate this concept, Figure 5 presents classifiers (DT, SVM, and ANN) derived from feature set 7. This approach is selected due to its use of only three features, making the visualization of the decision space more intuitive, particularly for SVM.

Figure 5(a) shows the DT, where thresholds are easily understood. For example, if the minimum fundamental magnitude of phase a (from STFT) is below 0.97, phase b is below 0.9, and phase c is below 0.89 (left side of the tree), it likely indicates a voltage sag caused by a three-phase fault (abcG). The interpretation here is straightforward since reduced magnitudes across all three phases suggest a fault affecting all phases, typically a three-phase fault. Even with larger trees for higher-dimensional spaces, the binary rule-based nature of DT makes thresholds and their physical interpretations clear.

Figure 5(b) illustrates the SVM, where a decision boundary clearly separates voltage sags resulting from three-phase faults (abcG) and two-phase-to-ground faults involving phases a and b (abG). While a physical interpretation similar to DT is possible, it is worth noting that only a portion of the SVM is illustrated for better visualization. The full quadratic SVM is more complex, using several decision boundaries to categorize the ten types of sags.

For the ANN, as shown in Figure 5(c), the interconnected layers of neurons reinforce its black-box nature. The model offers no meaningful insight into the physical interpretation of weights and neurons, underscoring its complexity and lack of interpretability.

Figure 5. Visualization of (a) DT, (b) SVM, and (c) ANN

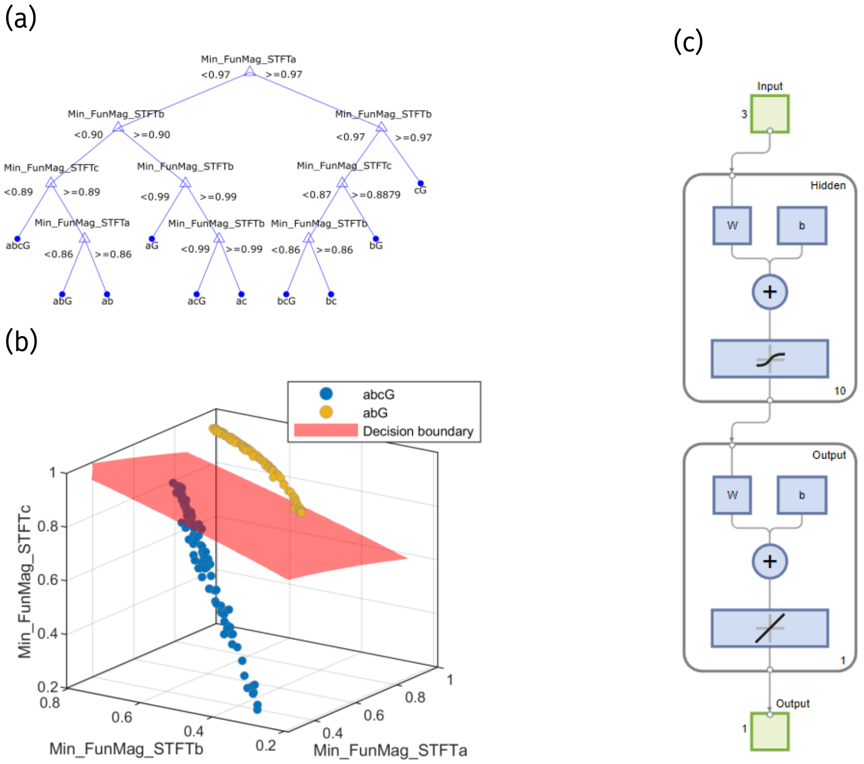

Source: own elaboration

While interpretability is inherently qualitative and lacks a direct numerical score, it is essential to quantify it for inclusion in the AHP-based evaluation. An overall interpretability score can be assigned to the classification approaches based on subjective criteria, including simplicity, transparency, and consistency. Each of these aspects is weighted equally. To calculate the overall interpretability score, individual scores for simplicity, transparency, and consistency are assigned to each approach on a scale from 0 to 1, and the average of these scores is computed. The results are summarized in Table 4. The following criteria are used to evaluate each aspect:

- **Simplicity:** This refers to how easily the model can be understood and applied. For DT, simplicity is measured by the depth of the tree or the number of rules, which makes them highly interpretable with a score of 1.0. SVM have moderate simplicity due to the complexity of kernels and the number of support vectors, scoring 0.4. ANN have low simplicity because of their complex structure with many layers and neurons, resulting in a score of 0.2.
- **Transparency:** This measures how understandable the internal mechanics of the model are. DT are highly transparent as their decision-making process is clear and straightforward, scoring 1.0. SVM are moderately transparent; while the decision boundary can be understood, non-linear kernels add complexity, giving a score of 0.7. ANN are less transparent due to their complex architecture, resulting in a score of 0.4.
- **Consistency:** This evaluates how well the model's decisions align with human reasoning or domain knowledge. DT demonstrate good consistency by producing similar decisions for similar cases, scoring 0.8. SVM show moderate consistency, with decision boundaries that generally respect domain-specific criteria but can be less predictable, scoring 0.5. ANNs have lower consistency due to their complexity and variability, achieving a score of 0.3.

Table 4. Interpretability scores for the AI algorithms for classification.

Classifier	Simplicity	Transparency	Consistency	Total interpretability score
DT	1.0	1.0	0.8	0.93
SVM	0.4	0.7	0.5	0.53
ANN	0.2	0.4	0.3	0.30

Source: own elaboration

Overall suitability for voltage sag classification

The overall suitability of classifiers for fault-induced voltage sag classification was evaluated using the AHP, a well-established Multi-Criteria Decision Making (MCDM) approach. AHP enables a structured comparison of multiple criteria by weighing performance metrics according to their relative importance, as outlined in [50, 51].

In this study, the AHP was specifically tailored for a case where the classifiers are intended for real-time applications. Given this context, the selected performance metrics include prediction time, model size, interpretability, accuracy, number of features, and training time. It is essential to highlight that prediction time and training time are treated independently in this analysis due to their differing impacts on real-time performance. Prediction time is critical for real-time applications, where rapid decision-making is required, while training time is less critical once the model is deployed. Similarly, the number of features and model size are evaluated separately to reflect their individual contributions to the efficiency and feasibility of the classifiers.

The weights assigned to each performance metric were determined through AHP by performing pairwise comparisons of relative importance, constructing a criteria matrix, and calculating eigenvector values, as prescribed by AHP and MCDM theory [50, 51]. The resulting weights are presented in Table 5.

Table 5. Weights assigned to performance metrics obtained through the AHP.

Performance metric	Weight
Prediction time	0.3675
Model size	0.2722
Interpretability	0.1297
Accuracy	0.1138
Number of features	0.0606
Training time	0.0562

Source: own elaboration

The weights in Table 5 prioritize prediction time as the most crucial factor, ensuring rapid responses to prevent equipment damage or interruptions. Model size is also important, especially for deployment on resource-constrained devices, where smaller models enhance processing efficiency. Interpretability is essential for understanding the decision-making process, particularly in industrial settings where validation and regulatory compliance are necessary. While accuracy is important, it is balanced against the need for speed and resource efficiency. The number of features and training time are less critical, focusing on model simplicity and minimizing training overhead.

To apply the AHP using the weights in Table 5, it is crucial to normalize the performance metrics. Normalization ensures that the metrics, which may have different scales or units, are comparable, allowing for a fair evaluation across all criteria. According to MCDM theory, various approaches can be used for normalization [50]. In this study, metrics where smaller values are preferable (e.g., prediction time, model size, interpretability, number of features, and training time) are normalized using (1). Conversely, metrics where higher values are better (e.g., accuracy) are normalized using (2).

$$Normalized\ value = \frac{Minimum\ value\ of\ criterion}{Value} \tag{1}$$

$$Normalized\ value = \frac{Value}{Maximum\ value\ of\ criterion} \tag{2}$$

Once normalized, the AHP-based methodology is applied to evaluate the 30 classification approaches formulated for fault-induced voltage sag classification, encompassing three types of classifiers (DT, SVM, and ANN), each trained with 10 distinct feature sets. The resulting scores are depicted in Figure 6, which provides a comparative visualization of the overall suitability of each approach.

Figure 6. AHP results for voltage sag classification approaches.

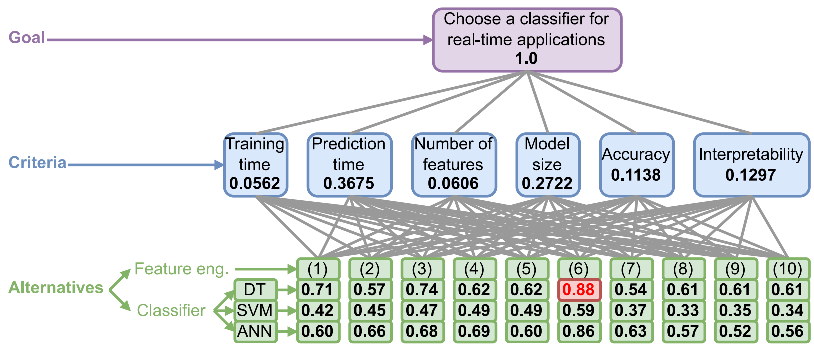

Source: own elaboration

Figure 6 shows that the approach employing DT with feature set 6, which leverages the DFT focusing on fundamental magnitude, phase angle, and THD, achieves the highest overall performance. This top-ranking score reflects an optimal balance across key metrics such as prediction time, model size, accuracy, and interpretability, making it particularly well-suited for real-time applications.

The radar chart in Figure 7 offers a comparison of the performance of the DT, SVM, and ANN classifiers, trained with feature set 6, across key metrics, further supporting the findings of the AHP analysis.

Figure 7. Radar chart of classifier performance metrics.

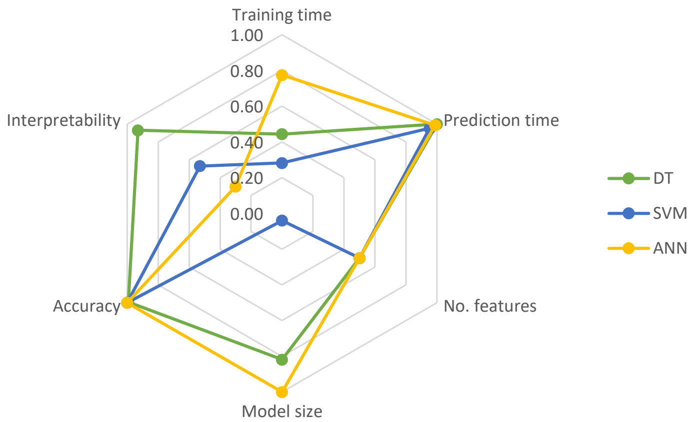

Source: own elaboration

Figure 7 shows that ANN excels in model size, offering the smallest memory footprint, making it ideal for resource-constrained devices. However, its lower interpretability is a significant drawback for real-time applications requiring transparency. DT stands out for its strong interpretability, rapid prediction times, and overall balance across metrics, confirming it as the best all-around choice for fault-induced voltage sag classification, especially where speed and clarity are crucial. SVM delivers competitive accuracy but is hindered by a larger model size and longer prediction times, reducing its efficiency and making it less optimal than DT for scenarios requiring quick responses and low computational overhead.

Conclusions

In this study, various machine learning techniques, including DT, SVM, and ANN, were evaluated for their effectiveness in classifying fault-induced voltage sags. The research involved generating extensive synthetic signals through MATLAB/Simulink simulations, applying feature engineering techniques, and conducting a systematic comparison using the AHP to assess performance across multiple criteria such as accuracy, computation time, storage requirements, and interpretability.

The findings demonstrate that DT are highly effective for fault-induced voltage sag classification, offering a combination of speed, accuracy, and interpretability that makes them ideal for real-time applications. Their straightforward decision-making process and low computational requirements make them particularly suitable for deployment in environments where both rapid response and resource efficiency are critical.

SVM also deliver good accuracy, though they require significantly more computational and storage resources. Their interpretability, while moderate, could be a limitation in applications where transparency and ease of understanding are important. However, SVM's robustness, particularly in handling complex classification tasks, suggests they may be better suited for scenarios where accuracy is paramount, and resource constraints are less critical.

ANN, while providing balanced performance across various metrics, fall short in interpretability. The complexity of their internal processes makes them less suitable for applications where understanding and explaining the decision-making process is crucial. Nonetheless, ANN may be beneficial in situations where model size and computational efficiency are the primary concerns, especially in resource-constrained environments.

Finally, the choice of classification techniques should be guided by the specific requirements of the application, including the need for real-time processing, resource availability, and the importance of interpretability. Future research should focus on expanding the evaluation criteria to include additional quantitative and qualitative metrics, and on developing methods to enhance the interpretability of classification results through Explainable Artificial Intelligence (XAI) techniques.

Acknowledgements

The authors gratefully acknowledge the financial support provided by the Oficina de Investigaciones (ODI) of the Universidad Distrital Francisco José de Caldas, Bogotá, Colombia, through the research project titled "A methodology for real-time detection and classification of power quality disturbances".

Bibliographics References

[1] J. E. Caicedo, D. Agudelo-Martínez, E. Rivas-Trujillo, and J. Meyer, "A systematic review of real-time detection and classification of power quality disturbances," Prot. Control Mod. Power Syst., vol. 8, no. 1, p. 3, 2023. DOI: https://doi.org/10.1186/s41601-023-00277-y.

[2] "Power Quality Measurements Methods, Testing and Measurement Techniques," IEC Std. 61000-4-30, 2019.

[3] M. H. J. Bollen, "What is power quality?," Electr. Power Syst. Res., vol. 66, no. 1, pp. 5–14, 2003. DOI: https://doi.org/10.1016/S0378-7796(03)00067-1.

[4] G. S. Chawda et al., "Comprehensive Review on Detection and Classification of Power Quality Disturbances in Utility Grid with Renewable Energy Penetration," IEEE Access, vol. 8, pp. 146807–146830, 2020. DOI: https://doi.org/10.1109/ACCESS.2020.3014732.

[5] M. Veizaga, C. Delpha, D. Diallo, S. Bercu, and L. Bertin, "Classification of voltage sags causes in industrial power networks using multivariate time-series," IET Gener. Transm. Distrib., 2023. DOI: https://doi.org/10.1049/gtd2.12765.

[6] É. M. Motoki, J. M. de C. Filho, P. M. da Silveira, N. B. Pereira, and P. V. G. de Souza, "Cost of Industrial Process Shutdowns Due to Voltage Sag and Short Interruption," Energies, vol. 14, no. 10, p. 2874, May 2021. DOI: https://doi.org/10.3390/en14102874.

[7] "IEEE Recommended Practice for Monitoring Electric Power Quality," 2019. DOI: https://doi.org/10.1109/IEEESTD.2019.8796486.

[8] J. E. Caicedo, E. Rivas, and J. Meyer, "Comparison of transformations and feature extraction techniques to characterize fault-induced voltage sags," Simp. Int. sobre la Calid. la Energía Eléctrica - SICEL, vol. 11, Jan. 2024. DOI: https://doi.org/10.15446/sicel.v11.110048.

[9] M. R. Alam, K. M. Muttaqi, and T. K. Saha, "Classification and Localization of Fault-Initiated Voltage Sags Using 3-D Polarization Ellipse Parameters," IEEE Trans. Power Deliv., vol. 35, no. 4, pp. 1812–1822, 2020. DOI: https://doi.org/10.1109/TPWRD.2019.2954857.

[10] L. F. A. Rodrigues, H. L. M. Monteiro, D. D. Ferreira, B. H. G. Barbosa, C. A. R. Junior, and C. A. Duque, "Sample-by-sample Power Quality Disturbance classification based on Sliding Window Recursive Discrete Fourier Transform," Electr. Power Syst. Res., vol. 235, p. 110607, Oct. 2024. DOI: https://doi.org/10.1016/j.epsr.2024.110607.

[11] I. S. Samanta et al., "A Comprehensive Review of Deep-Learning Applications to Power Quality Analysis," Energies, vol. 16, no. 11, p. 4406, May 2023. DOI: https://doi.org/10.3390/en16114406.

[12] R. Igual and C. Medrano, "Research challenges in real-time classification of power quality disturbances applicable to microgrids: A systematic review," Renew. Sustain. Energy Rev., vol. 132, p. 110050, Oct. 2020. DOI: https://doi.org/10.1016/j.rser.2020.110050.

[13] E. Perez-Anaya, A. Y. Jaen-Cuellar, D. A. Elvira-Ortiz, R. de J. Romero-Troncoso, and J. J. Saucedo-Dorantes, "Methodology for the Detection and Classification of Power Quality Disturbances Using CWT and CNN," Energies, vol. 17, no. 4, p. 852, Feb. 2024. DOI: https://doi.org/10.3390/en17040852.

[14] J. Li, Y. Yang, H. Lin, Z. Teng, F. Zhang, and Y. Xu, "A voltage sag detection method based on modified s transform with digital prolate spheroidal window," IEEE Trans. Power Deliv., vol. 36, no. 2, pp. 997–1006, 2021. DOI: https://doi.org/10.1109/TPWRD.2020.2999693.

[15] A. Bagheri, I. Y. H. Gu, M. H. J. Bollen, and E. Balouji, "A Robust Transform-Domain Deep Convolutional Network for Voltage Dip Classification," IEEE Trans. Power Deliv., vol. 33, no. 6, pp. 2794–2802, 2018. DOI: https://doi.org/10.1109/TPWRD.2018.2854677.

[16] L. Ramalingappa and A. Manjunatha, “Power quality event classification using complex wavelets phasor models and customized convolution neural network,” Int. J. Electr. Comput. Eng., vol. 12, no. 1, p. 22, Feb. 2022. DOI: https://doi.org/10.11591/ijece.v12i1.pp22-31.

[17] Y. Pu, H. Yang, X. Ma, and X. Sun, “Recognition of voltage sag sources based on phase space reconstruction and improved VGG transfer learning,” Entropy, vol. 21, no. 10, 2019. DOI: https://doi.org/10.3390/e21100999.

[18] Ç. Kocaman and M. Özdemir, “Determining five kinds of power quality disturbances by using statistical methods and wavelet energy coefficients,” Renew. Energy Power Qual. J., vol. 1, no. 15, pp. 745–750, 2017. DOI: https://doi.org/10.24084/repqj15.455.

[19] A. D. Gonzalez-Abreu, M. Delgado-Prieto, J. J. Saucedo-Dorantes, and R. A. Osornio-Rios, “Novelty detection on power quality disturbances monitoring,” Renew. Energy Power Qual. J., vol. 19, pp. 211–216, 2021. DOI: https://doi.org/10.24084/repqj19.259.

[20] W. L. Rodrigues Junior, F. A. S. Borges, R. de A. L. Rabelo, J. J. P. C. Rodrigues, R. A. S. Fernandes, and I. N. Silva, “A methodology for detection and classification of power quality disturbances using a real-time operating system in the context of home energy management systems,” Int. J. Energy Res., vol. 45, no. 1, pp. 203–219, Jan. 2021. DOI: https://doi.org/10.1002/er.5183.

[21] J. Xiu, X. Guangye, M. Xiangping, and D. Guilin, “Voltage sag detection method based on dq transform and complex wavelet transform,” in 2021 IEEE International Conference on Electrical Engineering and Mechatronics Technology, ICEEMT 2021, 2021, pp. 429–434. DOI: https://doi.org/10.1109/ICEEMT52412.2021.9602691.

[22] M. R. Alam, F. Bai, R. Yan, and T. K. Saha, “Classification and Visualization of Power Quality Disturbance-Events Using Space Vector Ellipse in Complex Plane,” IEEE Trans. Power Deliv., vol. 36, no. 3, pp. 1380–1389, 2021. DOI: https://doi.org/10.1109/TPWRD.2020.3008003.

[23] N. M. Khoa and D. D. Tung, “An extended Kalman filter for detecting voltage sag events in power systems,” J. Electr. Syst., vol. 14, no. 2, pp. 192–204, 2018, [Online]. Available: https://www.proquest.com/openview/17dc530e46e9e2bc3226e3dc476e9119/1?pq-origsite=gscholar&cbl=4433095

[24] H. Zhang et al., “Multi-strategy active learning for power quality disturbance identification,” Appl. Soft Comput., vol. 154, p. 111326, Mar. 2024. DOI: https://doi.org/10.1016/j.asoc.2024.111326.

[25] N. K. Swarnkar, O. P. Mahela, and M. Lalwani, “Multivariable signal processing algorithm for identification of power quality disturbances,” Electr. Power Syst. Res., vol. 221, p. 109480, Aug. 2023. DOI: https://doi.org/10.1016/j.epsr.2023.109480.

[26] P. K. Ray, H. K. Sahoo, A. Mohanty, J. K. Bhutto, A. B. Barnawi, and A. A. Alshaya, “Robust H-Infinity Filter and PSO-SVM Based Monitoring of Power Quality Disturbances System,” IEEE Access, vol. 12, pp. 39041–39057, 2024. DOI: https://doi.org/10.1109/ACCESS.2024.3367727.

[27] R. Mahla, B. Khan, O. P. Mahela, and A. Singh, “Recognition of complex and multiple power quality disturbances using wavelet

packet-based fast kurtogram and ruled decision tree algorithm," Int. J. Model. Simulation, Sci. Comput., vol. 12, no. 05, p. 2150032, Oct. 2021. DOI: https://doi.org/10.1142/S179396232150032X.

[28]A. Akbarpour, M. Nafar, and M. Simab, "Multiple power quality disturbances detection and classification with fluctuations of amplitude and decision tree algorithm," Electr. Eng., vol. 104, no. 4, pp. 2333–2343, Aug. 2022. DOI: https://doi.org/10.1007/s00202-021-01481-5.

[29]L. Chen, S. Chen, J. Xu, and C. Zhou, "Power quality disturbances identification based on deep neural network model of time-frequency feature fusion," Electr. Power Syst. Res., vol. 231, p. 110283, Jun. 2024. DOI: https://doi.org/10.1016/j.epsr.2024.110283.

[30]R. Machlev, M. Perl, J. Belikov, K. Y. Levy, and Y. Levron, "Measuring Explainability and Trustworthiness of Power Quality Disturbances Classifiers Using XAI—Explainable Artificial Intelligence," IEEE Trans. Ind. Informatics, vol. 18, no. 8, pp. 5127–5137, Aug. 2022. DOI: https://doi.org/10.1109/TII.2021.3126111.

[31] S. Akkaya, E. Yüksek, and H. M. Akgün, "A New Comparative Approach Based on Features of Subcomponents and Machine Learning Algorithms to Detect and Classify Power Quality Disturbances," Electr. Power Components Syst., vol. 52, no. 8, pp. 1269–1292, May 2024. DOI: https://doi.org/10.1080/15325008.2023.2260375.

[32]N. A. Shafiqa Zakaria, D. M. Said, N. Rosmin, N. Ahmad, M. S. Shah Jamil, and S. Mirsaeidi, "Comparison analysis of different classification methods of power quality disturbances," Int. J. Electr. Comput. Eng., vol. 12, no. 6, p. 5754, Dec. 2022. DOI: https://doi.org/10.11591/ijece.v12i6.pp5754-5764.

[33]C. I. Garcia, F. Grasso, A. Luchetta, M. C. Piccirilli, L. Paolucci, and G. Talluri, "A Comparison of Power Quality Disturbance Detection and Classification Methods Using CNN, LSTM and CNN-LSTM," Appl. Sci., vol. 10, no. 19, p. 6755, Sep. 2020. DOI: https://doi.org/10.3390/app10196755.

[34]J. C. Bravo-Rodríguez, F. J. Torres, and M. D. Borrás, "Hybrid Machine Learning Models for Classifying Power Quality Disturbances: A Comparative Study," Energies, vol. 13, no. 11, p. 2761, Jun. 2020. DOI: https://doi.org/10.3390/en13112761.

[35]G. Li, Z. Yu, B. Zheng, B. Qi, Z. Su, and D. Wang, "Voltage Sag Source Location based on the Random Forest," J. Phys. Conf. Ser., vol. 2584, no. 1, p. 012144, Sep. 2023. DOI: https://doi.org/10.1088/1742-6596/2584/1/012144.

[36]Y. Mohammadi, A. Salarpour, and R. Chouhy Leborgne, "Comprehensive strategy for classification of voltage sags source location using optimal feature selection applied to support vector machine and ensemble techniques," Int. J. Electr. Power Energy Syst., vol. 124, 2020. DOI: https://doi.org/10.1016/j.ijepes.2020.106363.

[37] E. A. Nagata et al., "Real-time voltage sag detection and classification for power quality diagnostics," Meas. J. Int. Meas. Confed., vol. 164, 2020. DOI: https://doi.org/10.1016/j.measurement.2020.108097.

[38]W. Jiekang and C. Xiaohua, "An identification method for voltage sag in distribution systems using SVM with Grey Wolf algorithm," Int. J.

Power Energy Syst., vol. 44, no. 10, 2024, DOI: https://doi.org/10.2316/J.2024.203-0434.

[39]K. Thirumala, S. Pal, T. Jain, and A. C. Umarikar, "A classification method for multiple power quality disturbances using EWT based adaptive filtering and multiclass SVM," Neurocomputing, vol. 334, pp. 265–274, 2019. DOI: https://doi.org/10.1016/j.neucom.2019.01.038.

[40] H. Sha, F. Mei, C. Zhang, Y. Pan, and J. Zheng, "Identification method for voltage sags based on K-means-singular value decomposition and least squares support vector machine," Energies, vol. 12, no. 6, 2019. DOI: https://doi.org/10.3390/en12061137.

[41]Z. Liu, Y. Cui, and W. Li, "A Classification Method for Complex Power Quality Disturbances Using EEMD and Rank Wavelet SVM," IEEE Trans. Smart Grid, vol. 6, no. 4, pp. 1678–1685, 2015. DOI: https://doi.org/10.1109/TSG.2015.2397431.

[42]Rahul and B. Choudhary, "An Advanced Genetic Algorithm with Improved Support Vector Machine for Multi-Class Classification of Real Power Quality Events," Electr. Power Syst. Res., vol. 191, 2021. DOI: https://doi.org/10.1016/j.epsr.2020.106879.

[43]S. Der Lu, H. W. Sian, M. H. Wang, and R. M. Liao, "Application of extension neural network with discrete wavelet transform and Parseval's theorem for power quality analysis," Appl. Sci., 2019. DOI: https://doi.org/10.3390/app9112228.

[44]I. S. Samanta, P. K. Rout, S. Mishra, K. Swain, and M. Cherukuri, "Fast TT transform and optimized probabilistic neural network-based power quality event detection and classification," Electr. Eng., vol. 104, no. 4, pp. 2757–2774, Aug. 2022. DOI: https://doi.org/10.1007/s00202-022-01505-8.

[45]V. Veeramsetty, A. Dhanush, A. Nagapradyullatha, G. R. Krishna, and S. R. Salkuti, "Power quality disturbances classification using autoencoder and radial basis function neural network," Int. J. Emerg. Electr. Power Syst., vol. 0, no. 0, Sep. 2023. DOI: https://doi.org/10.1515/ijeeps-2023-0143.

[46]S. . Suganthi, A. Vinayagam, V. Veerasamy, A. Deepa, M. Abouhawwash, and M. Thirumeni, "Detection and classification of multiple power quality disturbances in Microgrid network using probabilistic based intelligent classifier," Sustain. Energy Technol. Assessments, vol. 47, p. 101470, Oct. 2021. DOI: https://doi.org/10.1016/j.seta.2021.101470.

[47]O. Cortes-Robles, E. Barocio, A. Obushevs, P. Korba, and F. R. S. Sevilla, "Fast-training feedforward neural network for multi-scale power quality monitoring in power systems with distributed generation sources," Measurement, vol. 170, p. 108690, Jan. 2021. DOI: https://doi.org/10.1016/j.measurement.2020.108690.

[48] H. Liu, F. Hussain, S. Yue, O. Yildirim, and S. J. Yawar, "Classification of multiple power quality events via compressed deep learning," Int. Trans. Electr. Energy Syst., 2019. DOI: https://doi.org/10.1002/2050-7038.12010.

[49]Q. Xu et al., “Efficient Identification Method for Power Quality Disturbance: A Hybrid Data-Driven Strategy,” Processes, vol. 12, no. 7, p. 1395, Jul. 2024. DOI: https://doi.org/10.3390/pr12071395.

[50]M. Shao, Z. Han, J. Sun, C. Xiao, S. Zhang, and Y. Zhao, “A review of multi-criteria decision-making applications for renewable energy site selection,” Renew. Energy, vol. 157, pp. 377–403, Sep. 2020. DOI: https://doi.org/10.1016/j.renene.2020.04.137.

[51]Y. Chen et al., “A Novel Approach for Evaluating Power Quality in Distributed Power Distribution Networks Using AHP and S-Transform,” Energies, vol. 17, no. 2, p. 411, Jan. 2024. DOI: https://doi.org/10.3390/en17020411.